SPATIAL TEMPORAL CONDITION OF RECENT SEISMICITY IN THE NORTHERN PART OF SUMATRA

Inna Nurana[*], Andrean V. H. Simanjuntak[**], Muksin Umar[***], Djati Cipto Kuncoro[****], Syamsidik[***], Yusran Asnawi[*****]

[*]*Graduate School of Mathematics and Applied Science, Universitas Syiah Kuala, Banda Aceh, Indonesia*
[*]*Badan Meteorologi Klimatologi dan Geofisika (BMKG), Aceh, Indonesia, inna.nurana2604@gmail.com*
[**]*Badan Meteorologi Klimatologi dan Geofisika (BMKG), Aceh, Indonesia*
[**]*Tsunami Disaster Mitigation and Research Center (TDMRC), Universitas Syiah Kuala (USK), Aceh, Indonesia, andreansimanjuntak@gmail.com*
[***]*Tsunami Disaster Mitigation and Research Center (TDMRC), Universitas Syiah Kuala (USK), Aceh, Indonesia, muksin.umar@unsyiah.ac.id, syamsidik@tdmrc.org*
[****]*Badan Meteorologi Klimatologi dan Geofisika (BMKG), Aceh, Indonesia, dckuncoro@gmail.com*
[*****]*Education of Information Technology Department, Universitas Islam Negeri Ar-Raniry, Aceh, Indonesia, yusran@ar-raniry.ac.id*

Email Correspondence: andreansimanjuntak@gmail.com

Received : January 28, 2021 Accepted : April 29, 2021 Published : June 30, 2021

Abstract: The condition of stress and recent seismicity in the seismic-prone area can be statistically analyzed with the Gutenberg-Richter relation ($Log\ N = a - bM$). We apply this relation to the hypocenter distribution for the period 1970-2020 with M ≥ 4 and depth ≤ 100 km in the northern part of Sumatra. Spatially, The results obtained *a*-values and *b*-values that figure a lateral heterogeneity and stress accumulation at the interface zone in the subduction system and the northern segmentation of the Seulimeum fault. In time, both zones illustrate a slow time-to-failure cycle and the seismic gap with high-stress accumulation in the specific clusters with high parameter values. The results of the spatial-temporal analysis illustrate that a low statistical parameter value usually precedes each major earthquake event.
Keywords : seismic statistic, seismic stress, subduction, seulimeum, *a*-value, *b*-value

Abstrak: Kondisi stress dan seismisitas terkini di daerah rawan gempa dapat dianalisis secara statistik dengan hubungan Gutenberg-Richter ($Log\ N = a - bM$). Kami memakai hubungan ini pada distribusi hiposenter pada periode 1970 - 2020 dengan M ≥ 4 dan kedalaman ≤ 100 km di bagian utara Sumatera. Secara spasial, hasil yang diperoleh yaitu nilai-a dan nilai-b yang menggambarkan heterogenitas lateral dan akumulasi stress pada zona pertemuan di sistem subduksi dan segmentasi utara dari sesar Seulimeum. Secara waktu, kedua wilayah menggambarkan siklus *time-to-failure* yang lambat dan zona *seismic-gap* dengan akumulasi stress yang tinggi pada kluster tertentu dengan nilai parameter yang tinggi. Hasil analisis spasial temporal menggambarkan bahwa setiap kejadian gempa besar biasanya didahului dengan nilai parameter statistik yang rendah.
Kata kunci : statistik kegempaan, stress seismik, subduksi, seulimeum, nilai-a, nilai-b

Recommended APA Citation :

Nurana, I., Simanjuntak, A. V. H., Umar, M., Kuncoro, D. C., Syamsidik, & Asnawi, Y. (2021). Spatial Temporal Condition of Recent Seismicity In The Northern Part of Sumatra. *Elkawnie*, *7*(1), 131-145. https://doi.org/10.22373/ekw.v7i1.8797

Introduction

The northernmost part of Sumatra stands on the active tectonic system, as shown in figure 1, and conveniently generates earthquakes (McCaffrey, 2009, Meng *et al.,* 2012, Qiu *et al.,* 2018, Craig & Copley, 2018, Fujii *et al.,* 2020). Oblique subduction between Indo-Australia plate with a slip rate of 5 mm/yr beneath Eurasian generates the oceanic earthquake (Bradley *et al.,* 2017; Liu *et al.,* 2018). Several historical earthquakes that followed by a tsunami, such as 2004 Sumatra-Andaman M 9.0 (Lay *et al.,* 2005, Khan *et al.,* 2020), 2005 Nias M 8.5 (Meltzner *et al.,* 2015), and 2012 Wharton Basin M8.2 and 8.1 (Hill *et al.,* 2015).

While, the land earthquake is generated by an active segment in the Sumatra Fault System with a slip rate of 10-20 mm/yr (Genrich *et al.,* 2000, Sieh & Natawidjaja 2000, Ito *et al.,* 2012, Salman *et al.,* 2020). The historical events, such as 1964 Seulimeum M 6.4 (Hurukawa & Biana, 2013), 1996 Kutacane M 6.1 (Simanjuntak *et al.,* 2018), 2013 Bener Meriah M 6.3 (Gunawan et al., 2018, Muksin *et al.,* 2019), 2017 Pidie Jaya M 6.5 (Muzli *et al.,* 2018, Simanjuntak *et al.,* 2019; Qadariyah *et al.,* 2018, Idris *et al.,* 2019, Pasari *et al.,* 2021).

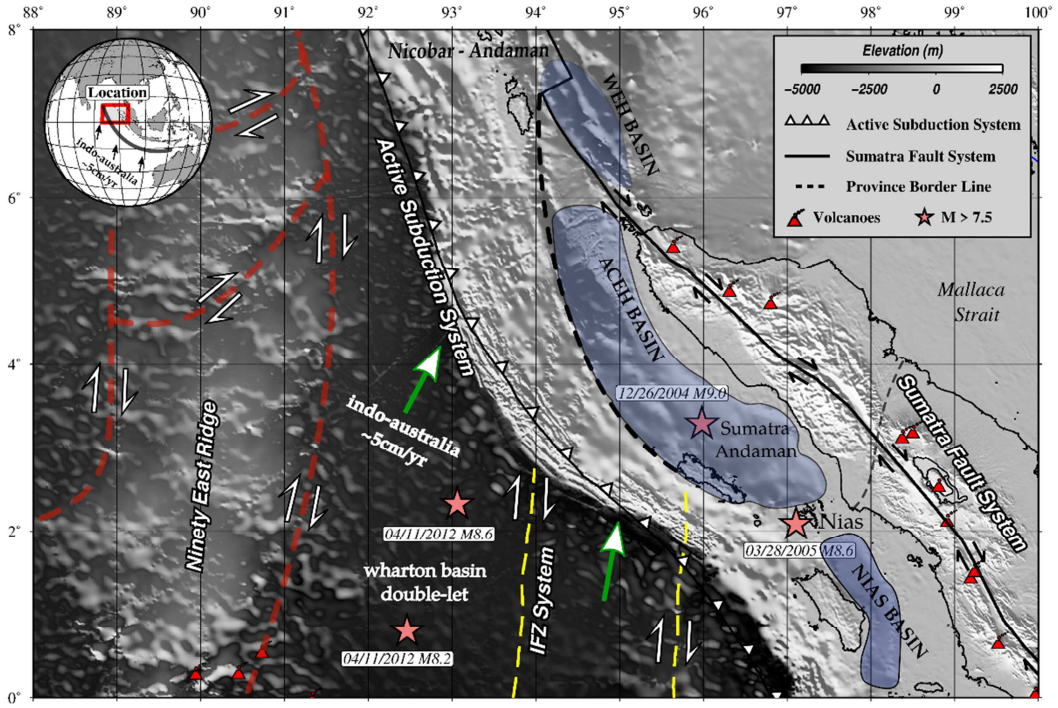

Figure 1. A tectonic map of the northernmost part of Sumatra illustrates a geological structure with Ninety East ridge in the eastern part, an active subduction system along the coastal line, and a Sumatra fault system.

Several studies have been studied to explain the tectonic process in the study area, for example, seismic hazard (Omang *et al.,* 2017, Simanjuntak *et al.,* 2020), detailed structure (Lange *et al.,* 2018, Muksin *et al.,* 2019), geodetic (Gunawan *et al.,* 2019) and tsunami (Syamsidik *et al.,* 2018). Moreover, an updated study must be continuously conducted to explain the recent seismicity in

the spatial and temporal conditions. In this research, we conduct a seismic statistical analysis to explain the recent seismicity in the period of 1970 - 2020 with magnitude ≥ 4.

Then, we separated the data in the time clustering before and after the 2004 earthquake as the major earthquake. Then, the formula of Gutenberg-Richter (1944) is used to explain the relationship between frequency and earthquake magnitude ($Log\ N = a - bM$). The study area is divided into 0.5º x 0.5º bins for spatial analysis. Many seismicity studies have been globally studied with the Gutenberg-Ritcher method, for example, nowcasting earthquake (Pasari., 2019), forecasting earthquake (Toda *et al.,* 2020), induced seismicity (Ellsworth., 2013).

In this research, we perform the statistical parameter in spatial and temporal conditions for recent seismicity in the northern part of Sumatra. The results show the three zones in the northern, southern, and center parts located in the interface zone of subduction have high a and b-value. The high value can be assumed as the time-to-failure cycle that has the potential to release stress in the future from major earthquake.

High values are also associated with the 2004 earthquake rupture, while an active fault influences the center part. In addition, our statistical calculation can highlight updated seismicity that is influenced by the last activity as the earthquake cycle. Furthermore, this research can be used as information for disaster mitigation programs and complement the tectonic reference based on updated spatial-temporal seismicity.

Data and Method

In this study, hypocenter data (see. Fig. 2) were combined from the International Seismological Center (ISC) and Badan Meteorologi Klimatologi dan Geofisika (BMKG) with M ≥ 4 and depth ≤ 100 km in a period of 1970-2020. Hypocenter data before 2009 was fully derived from ISC (International Seismic Center) bulletin. The data is already well-relocated and teleseismically well-constrained (Engdahl *et al.,* 2020). ISC bulletin data are quite widely used in much seismic analysis, such as seismic hazard (Irwandi *et al.,* 2021, Simanjuntak & Olymphia, 2017), regional tomography (Hist *et al.,* 1991, Zhao, 2004, Koulakov *et al.*, 2015), mantle structure and discontinuities (Lu *et al.,* 2019; Khrepy *et al.,* 2016), and etc.

In addition, data for 2010 - 2020 were obtained from BMKG (Badan Meteorologi Klimatologi dan Geofisika) as the official Indonesian geophysics agency. BMKG was starting comprehensive seismic monitoring from 2008 until now. The result monitoring has compiled all well-analyzed events from various sources and mechanisms. There is four majors earthquake in the last decade occurred in the study area and trigger some earthquakes that occurred in the unknown fault due to high stress release.

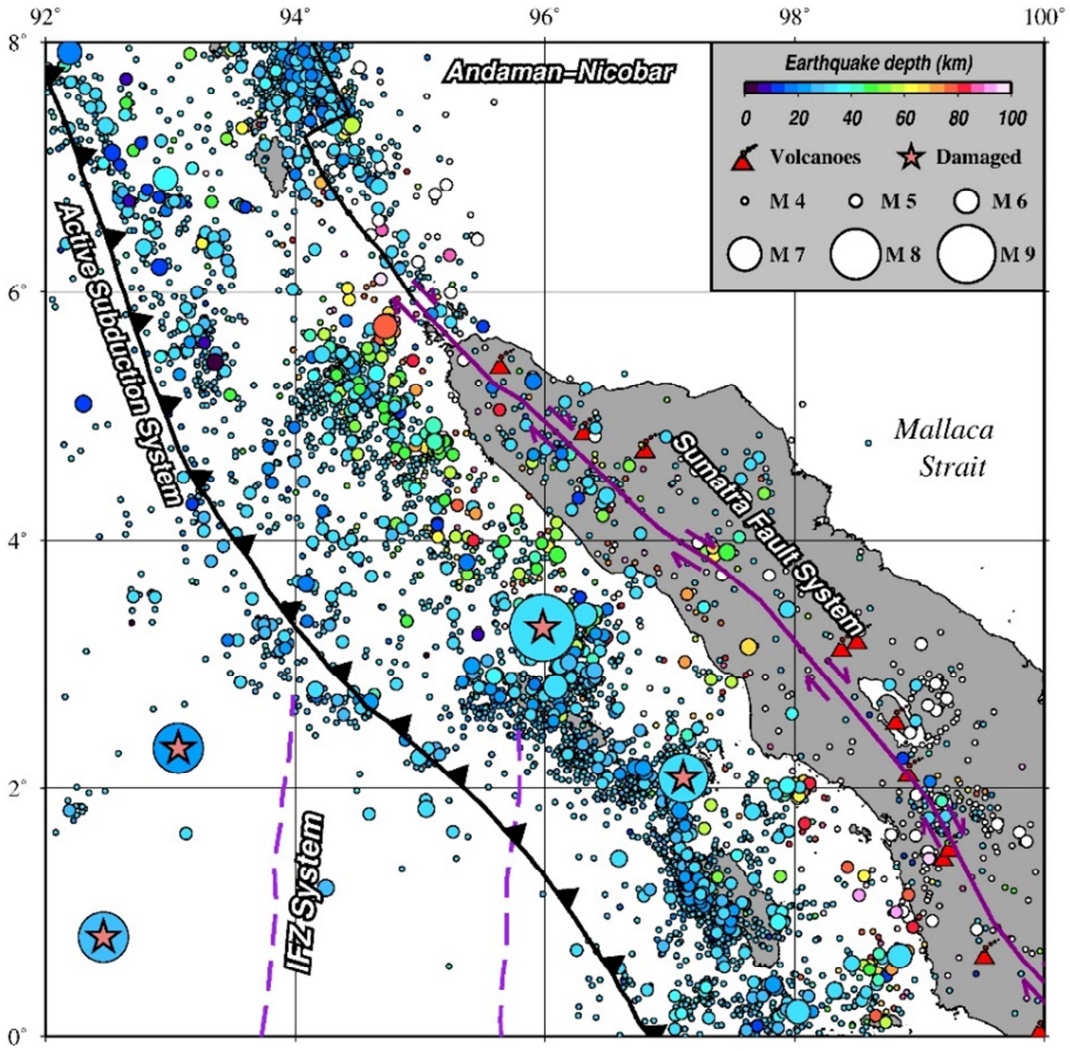

Figure 2. Earthquake distribution map in the study area in the period of 1970 – 2020 with magnitude range ≥ 4 (pink star as a sign of damaged earthquake) and depth range of 0 – 100 km.

Method

Physically, the nature of earthquake is a complicated case and not simply homogeneous in space and time (Zhuang *et al.,* 2002, Kagan, 2004, Langenbruch *et al.,* 2018). Therefore, a series of earthquake occurrences are needed to understand the natural process (Hainzl, 2016, Mueller, 2019). The earthquake series is generally followed by stress release, as a time-to-failure cycle, and can be explained as a statistical method (Hardebeck & Okada, 2018), as shown in fig 3.

We used a well-established relationship known as Gutenberg-Richter (1944) to relate the recent seismicity with updated geophysical information. This relationship is calculated in the exponential formula between magnitude and frequency earthquake as the following this equation:

$$\boldsymbol{log\ N = a - b\ M} \quad \text{.....(1)}$$

Statistical methods are routinely used to highlight the earthquake seismicity condition in the time-space-magnitude relationship based on the earthquake hypocenter catalog (Davidsen *et al.,* 2006). *N* is the cumulative number of earthquakes with a magnitude greater than or equal to *M*. The value of a is a seismic parameter that indicates the level of seismicity in the specific area (Wesnousky, 1994).

In comparison, the *b*-value is a statistical parameter that explains the tectonic characteristics in the specific area. Furthermore, the *b*-value describes the relationship between earthquake frequency and the stress level and the fragility of the rock in a place. To calculate the *b*-value, the likelihood method is used like the following equation

$$\boldsymbol{b} = \frac{\boldsymbol{log\ e}}{\bar{\boldsymbol{M}} - \boldsymbol{M_{min}}} = \frac{\boldsymbol{0.4343}}{\bar{\boldsymbol{M}} - \boldsymbol{M_{min}}} \quad \text{.....(2)}$$

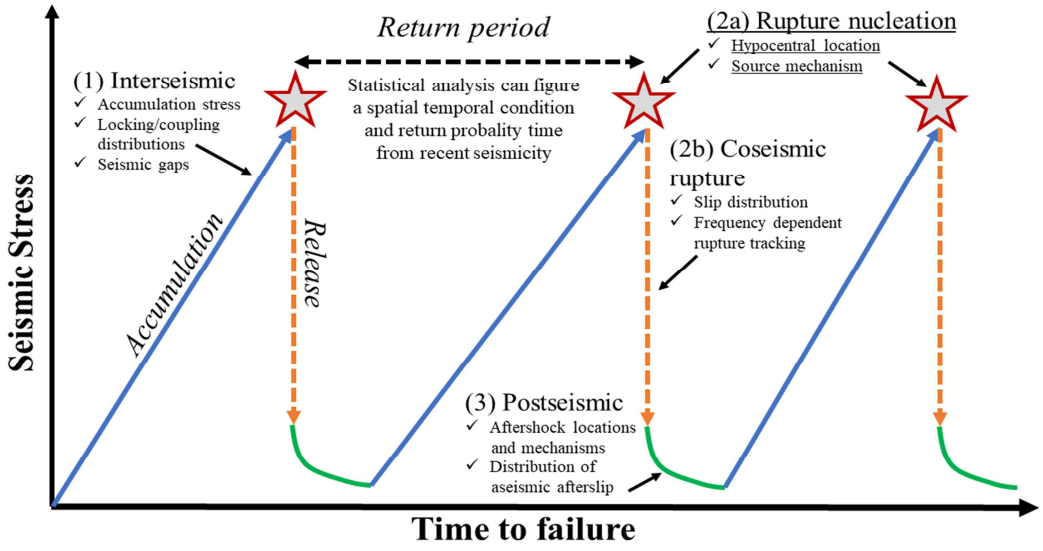

Figure 3. A schematic cartoon that illustrates a time-to-failure cycle for earthquakes return period when interseismic, coseismic and postseismic occurred in the stress release and time relationship. The accumulation and reslease follow the seismic stress change that increase in the interseismic and decrease when in the postseismic as a sign for a possible reccurence in the future.

$\bar{\boldsymbol{M}}$ is the average of magnitude and $\boldsymbol{M_{min}}$ is the minimum magnitude in the historical earthquake data. Then, *a*-value can be calculated by using the following equation (Wesnousky, 1994) :

$$\boldsymbol{a} = \boldsymbol{\log(N) + \log(b \ln 10) + M_{min} b} \quad \text{.....(3)}$$

In this research, the compiled data (see Fig. 4) is divided with a grid size of 0.5º x 0.5º to provide a more detailed spatial and temporal variation. Each grid

is assumed as the one cluster that has a similar source type and mechanism. Then, the statistical parameter was calculated for all earthquakes in each cluster.

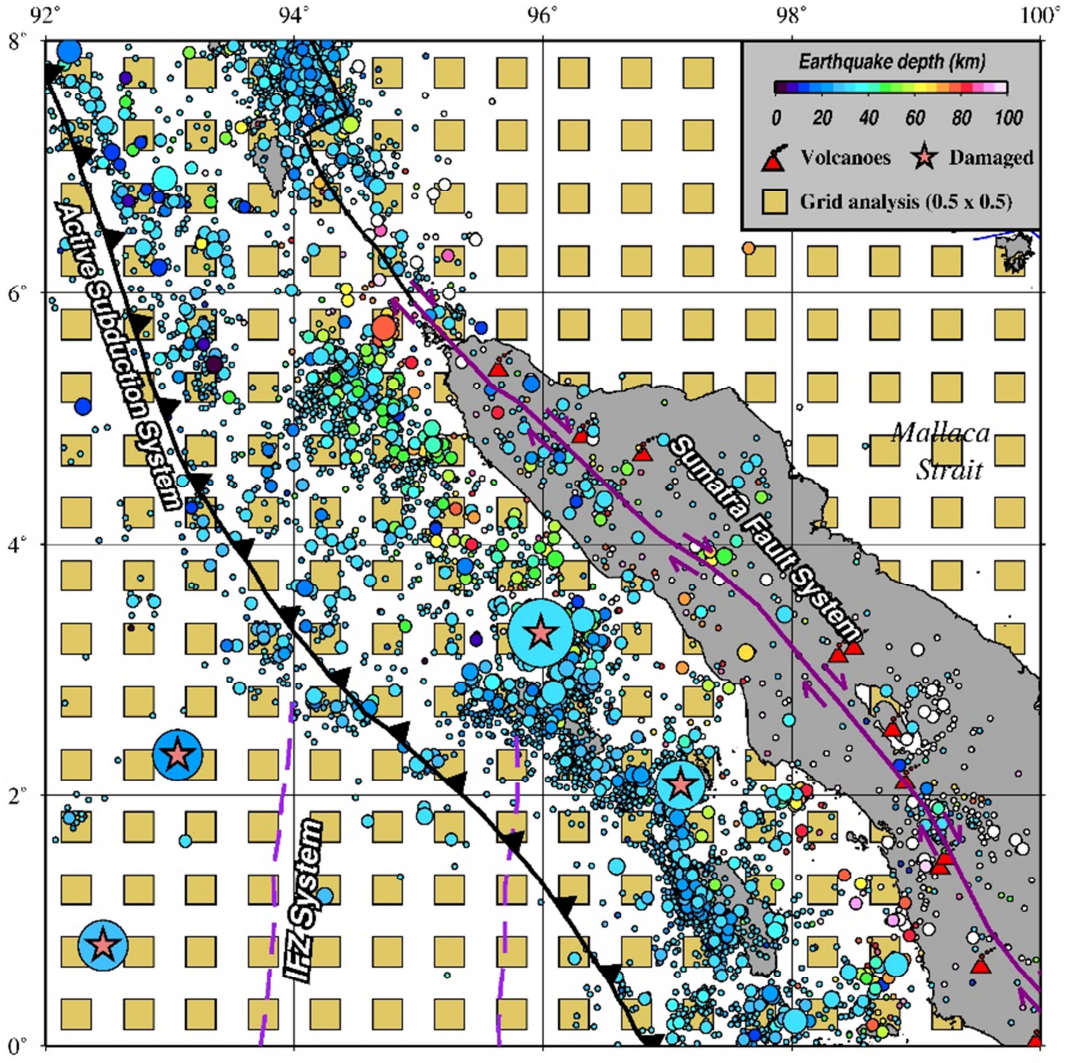

Figure 4. Grid cluster for all earthquakes with 0.5º x 0.5º bin for spatial analysis in the study area. The depth earthquakes are ranging from 0 – 100 km. Red stars are the big earthquake in Indian Ocean in this last decade.

Spatially, the output parameter will be interpolated to figure the variation that correlates to the big phenomena earthquake. In time, we figure the earthquake activity in the graph to provide a time-to-failure cycle pattern.

Result and Discussion

The spatial results (see Fig.5) show the earthquakes in 1970-2020 have a high *b*-value in the three locations. These areas are located in Simeuleu, the western part of Banda Aceh, and Sabang Island. The *b*-value is relevant with seismicity conditions that show low seismicity has an increasing parameter. The increasing parameter indicates a time-to-failure cycle with high-stress

accumulation and the existence of heterogeneity in the earthquake source properties (Baba *et al.,* 2020].

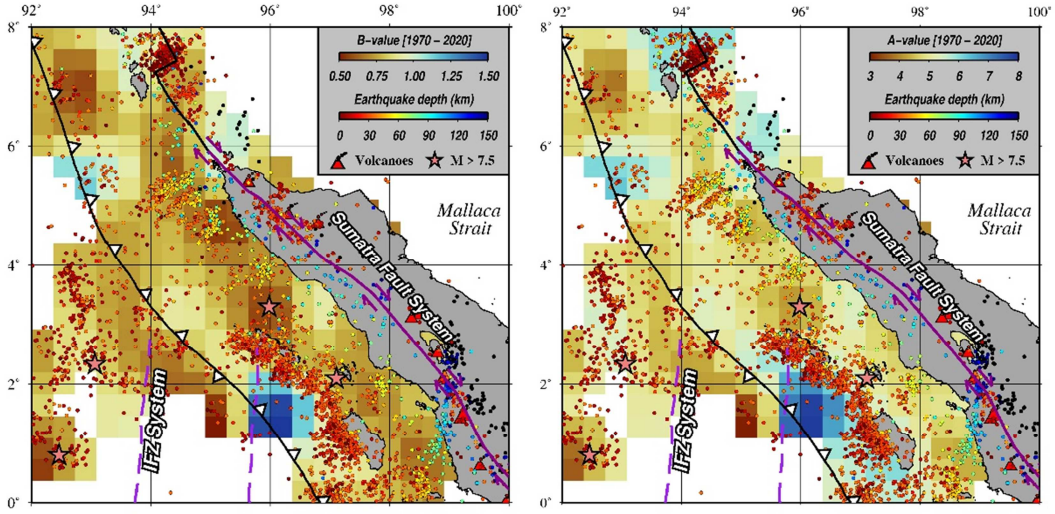

Figure 5. Spatial results of *b*-value (a) dan *a*-value (b) in the study area from 1970 to 2020.

On the other hand, the *a*-value with a range of 3 - 8 is located in the low seismicity zone. From figure 5, the high *a*-value has the same location as the *b*-value that indicates low seismicity followed by high-stress accumulation (Meltzner *et al.,* 2015). Furthermore, we compared the result of the historical earthquake before (see fig. 6) and after (see fig. 7) Andaman-Sumatera 2004 and Nias 2005 tsunami. The comparison performs connectivity between big earthquake phenomena and recent seismicity.

Spatial variation for earthquakes in 1970-2005

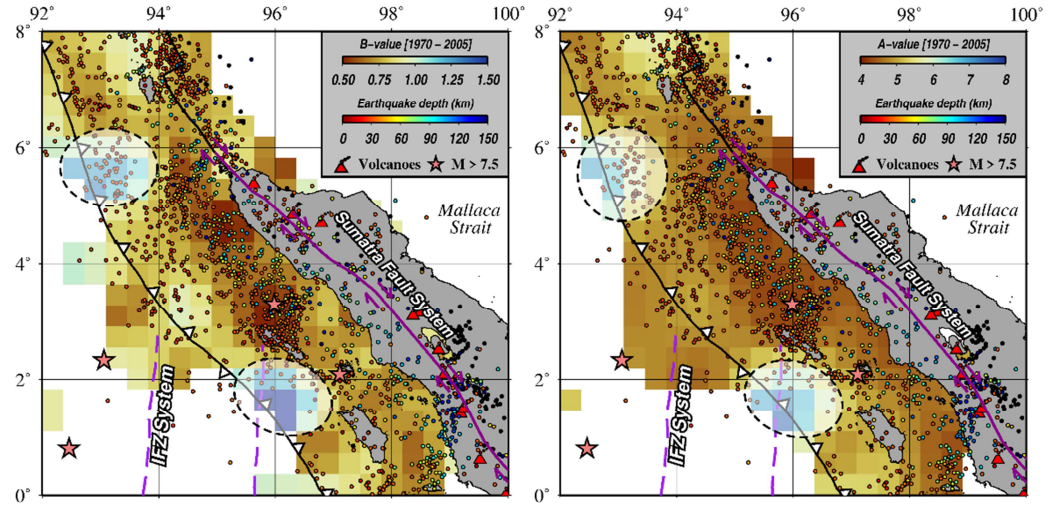

Figure 6. Spatial results of *b*-value (a) dan *a*-value (b) in the study area in the periods of 1970 – 2005.

From figure 6, the spatial result presents the statistical result with high parameters in the subduction zone. Two locations associate with low seismicity

and accumulate the stress release. The two locations are located in the north-eastern and southern parts of the interface zone. Both locations give the same result of b-value with a range of 1.25 – 1.5 and a-value with a 7 - 8. The grid also influences the result with bin 0.5º x 0.5º in the study area. The low seismicity can be categorized as a slow cycle time-to-failure cluster. The cycle is influenced by heterogenity conditions in the asperity zone that can accumulate seismic stress.

With high-stress accumulation, the subduction zone generated two big earthquakes in 2004 and 2005. The stress release can be assumed as the accumulation of significant global seismic events across century-scale periods. Meanwhile, the 2005 Nias earthquake with M 8.5, which occurred on the off coast of Sumatran island, is not categorized as an aftershock, despite its proximity to the epicentre (Dewey *et al.,* 2007). The 2005 Nias earthquake was most likely triggered by stress release, associated with the 2004 earthquake (Hughes *et al.,* 2010, Hsu *et al.,* 2010).

Spatial variation for earthquakes in 2006 - 2020

After 2004 and 2005, some seismic events have occurred in the unknown active zone that needs to be continuously updated for tectonic reference (Peña *et al.*, 2020). The massive stress release from the 2004 and 2005 earthquakes has triggered many active zones onshore and offshore. Then, we analyse the historical events in 2006 - 2020 with a statistical method. Figure 7 also figures the area with high parameters in the subduction zone, especially in the interface zone.

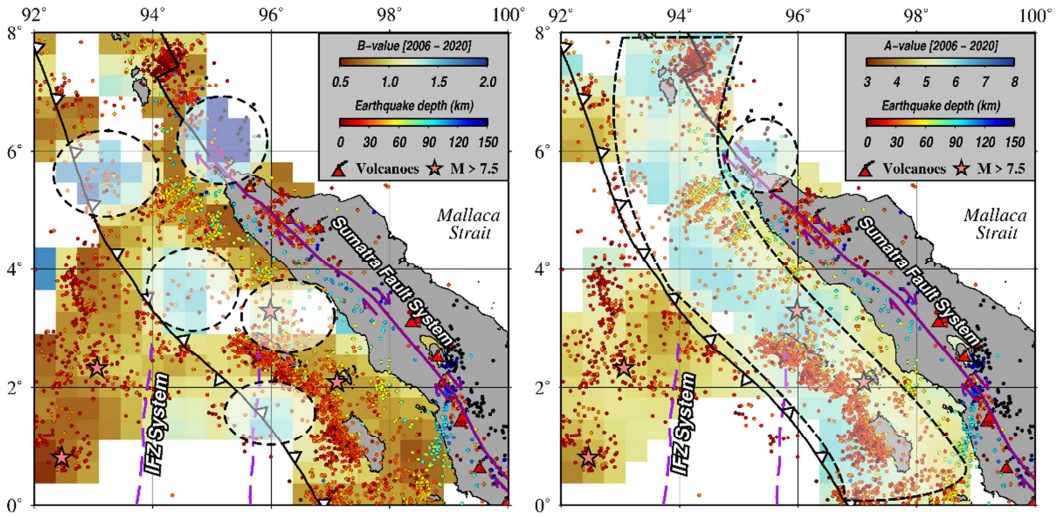

Figure 7. Spatial results of *b*-value (a) dan *a*-value (b) in the study area in the period of 2006 – 2020.

Furthermore, we figure five-zone with a high *b*-value which is totally different from the result for earthquakes before 2006. There are three zones in the interface zone and one zone in the 2004 earthquake rupture area with low seismicity. Stress conditions influence the low seismicity in the Earth's crust. The earthquakes can change the stress field as they relieve and redistribute the stresses

that have built up during the interseismic period (Sieh *et al.,* 2008). The interseismic period is different along the fault line in the seismic cycle. Various rupture area causes that occurred with different source properties (Pasari., 2019).

There is an active fault line with low seismicity in the northern part and gives a high statistical parameter. The fault can be assumed as the north segmented part of the Seulimeum fault in the sea and has a low-stress release. The low-stress release is influenced by long-term slip rate and displacement accumulation governed by fault system geometry (Sgambato *et al.,* 2020).

On the other hand, the *a*-value figure a homogenous spatial pattern along the northern coastline of Sumatra. The homogenous spatial condition is mostly located in the low seismicity zone in the subduction system (Tsang *et al.,* 2015). The a-value indicates low seismicity after big earthquake phenomena. On the contrary, an active earthquake cluster near Simelue island was formed in 2006-2020, while the cluster was not active before the big earthquake phenomena.

Temporal variation of all earthquakes in 1970-2020

We also perform a temporal analysis that shows the *b*-value is relatively low before the big earthquake phenomena (Sumatra-Andaman 2004 and Nias 2005) in fig.8.

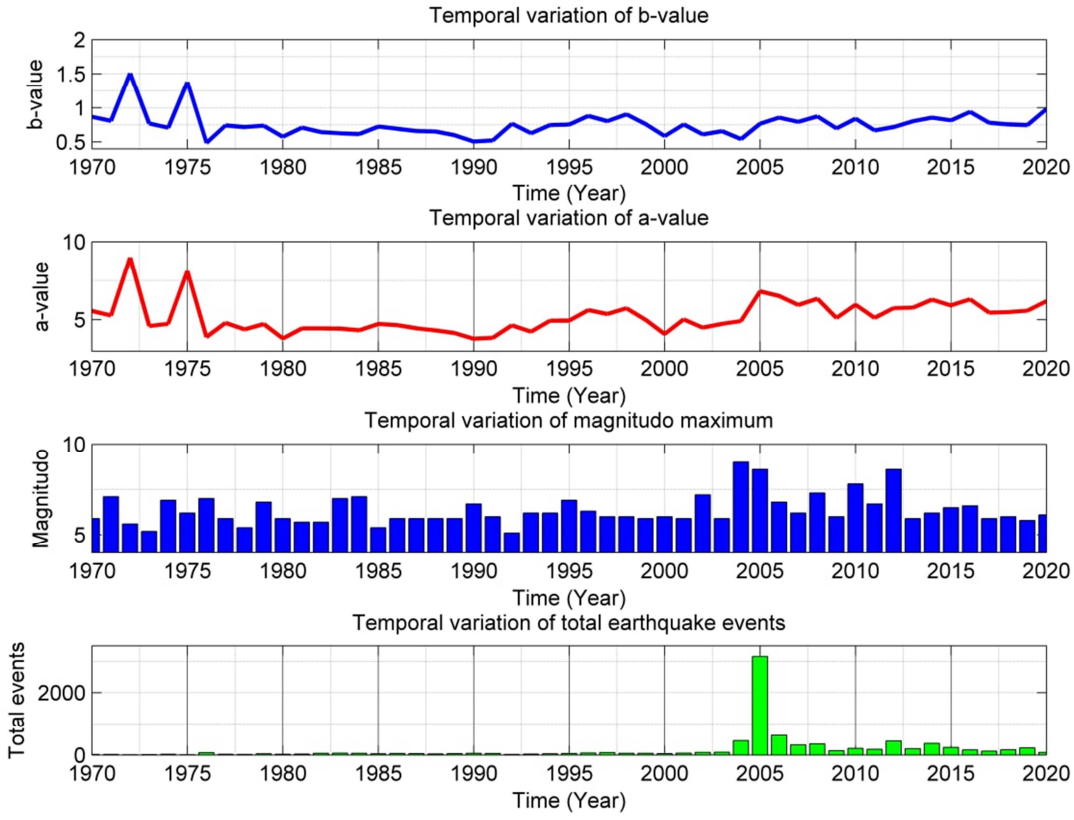

Figure 8. Graph of b-value, a-value, maximum magnitude, and earthquake temporal frequency for recent seismic ativity in the study area.

The low *b*-value indicates the area has high resistance in the asperity area to release the stress. In time, the resistance produces an accumulation of energy that periodically will release in the earthquake occurrence. Furthermore, the accumulation will release because of exceeded the elasticity limit of the rock in the rupture area that has a heterogeneity lateral (Davies *et al.,* 2012, Huang, 2018).

Historically, the results figure that every major earthquake is mostly preceded by a low b-value that follows a time-to-failure cycle (Pasari., 2019). The data before 2004 and 2005 can be categorized as the interseismic phase. The same pattern is also performed in the temporal result of a value. In 2005, a high a-value indicated massive seismic activity 2005 that generate the Nias earthquake with M 8.5. The parameter of *b*-value and *a*-value have decreased significantly since 2016 and slowly increase in 2020.

There is a possibility that the research area during the decline is collecting earthquake energy, and someday after reaching the limit of elasticity, the rock can come off again. Moreover, this study successfully provides an important updated condition of earthquake activities in the northern part of Sumatra, which is needed for mitigation concept and study in the future.

Conclusion

As we mentioned above, we figure that the seismicity in the northern part of Sumatra is quietly high and needs an updated study to explain seismicity in spatial and temporal conditions. The conclusions of this study are as follows:
Statistical parameters such as *a*-value and *b*-value figure the heterogenity lateral with a solid structure in the interface zone of subduction system and northern segmentation of Seulimeum fault. Both indicate a slow time-to-failure cycle with highly stress accumulated in the specific cluster. On the other hand, the analysis of the spatial result figures a different condition before and after 2004 and 2005 big earthquake that constructs a triggered pattern by stress release. Spatially, the high parameter results show two clusters of *a*-value and *b*-value in 1970-2005 while five clusters *b*-value and homogenous *a*-value in the subduction system in 2006 - 2020. The temporal analysis figures some major earthquake is mostly preceded by low statistical parameters that follow a time-to-failure cycle as the interseismic phase. Furthermore, this research can be connected to the stress seismic analysis based on earthquake mechanisms for comprehensive study.

References

Baba, S., Takemura, S., Obara, K., & Noda, A. (2020). Slow earthquakes illuminating interplate coupling heterogeneities in subduction zones. *Geophysical Research Letters*, 47(14), e2020GL088089.

Bradley, K. E., Feng, L., Hill, E. M., Natawidjaja, D. H., & Sieh, K. (2017). Implications of the diffuse deformation of the Indian Ocean lithosphere for

slip partitioning of oblique plate convergence in Sumatra. *Journal of Geophysical Research: Solid Earth*, 122(1), 572-591.

Craig, T. J., & Copley, A. (2018). Forearc collapse, plate flexure, and seismicity within the downgoing plate along the Sunda Arc west of Sumatra. *Earth and Planetary Science Letters*, 484, 81-91.

Davidsen, J., Grassberger, P., & Paczuski, M. (2006). Earthquake recurrence as a record breaking process. *Geophysical Research Letters*, 33(11).

Davies, T. R., McSaveney, M. J., & Boulton, C. J. (2012). Elastic strain energy release from fragmenting grains: Effects on fault rupture. *Journal of Structural Geology*, 38, 265-277.

Dewey, J. W., Choy, G., Presgrave, B., Sipkin, S., Tarr, A. C., Benz, H., ... & Wald, D. (2007). Seismicity associated with the Sumatra–Andaman Islands earthquake of 26 December 2004. *Bulletin of the Seismological Society of America*, 97(1A), S25-S42.

Ellsworth, W. L. (2013). Injection-induced earthquakes. *Science*, 341(6142).

Fujii, Y., Satake, K., Watada, S., & Ho, T. C. (2020). Slip distribution of the 2005 Nias earthquake (M w 8.6) inferred from geodetic and far-field tsunami data. *Geophysical Journal International*, 223(2), 1162-1171.

Genrich, J. F., Bock, Y., McCaffrey, R., Prawirodirdjo, L., Stevens, C. W., Puntodewo, S. S. O., ... & Wdowinski, S. (2000). Distribution of slip at the northern Sumatran fault system. *Journal of Geophysical Research: Solid Earth*, 105(B12), 28327-28341.

Gunawan, E., Widiyantoro, S., Meilano, I., & Pratama, C. (2019). Postseismic deformation following the 2 July 2013 Mw 6.1 Aceh, Indonesia, earthquake estimated using GPS data. *Journal of Asian Earth Sciences*, 177, 146-151.

Gutenberg, B. and C. F. Richter (1944). Frequency of earthquakes in California, *Bull. Seism. Soc. Am*. 34, 185-188.

Hainzl, S. (2016). Rate-dependent incompleteness of earthquake catalogs. *Seismological Research Letters*, 87(2A), 337-344.

Hardebeck, J. L., & Okada, T. (2018). Temporal stress changes caused by earthquakes: A review. *Journal of Geophysical Research: Solid Earth*, 123, 1350–1365.

Hill, E. M., Yue, H., Barbot, S., Lay, T., Tapponnier, P., Hermawan, I., ... & Sieh, K. (2015). The 2012 Mw 8.6 Wharton Basin sequence: A cascade of great earthquakes generated by near-orthogonal, young, oceanic mantle faults. *Journal of Geophysical Research: Solid Earth*, 120(5), 3723-3747.

Hsu, Y. J., Simons, M., Avouac, J. P., Galetzka, J., Sieh, K., Chlieh, M., ... & Bock, Y. (2006). Frictional afterslip following the 2005 Nias-Simeulue earthquake, Sumatra. *Science*, 312(5782), 1921-1926.

Huang, Y. (2018). Earthquake rupture in fault zones with along-strike material heterogeneity. *Journal of Geophysical Research: Solid Earth*, 123(11),

9884-9898.

Hurukawa, N., Wulandari, B. R., & Kasahara, M. (2014). Earthquake history of the Sumatran fault, Indonesia, since 1892, derived from relocation of large earthquakes. *Bulletin of the Seismological Society of America*, 104(4), 1750-1762.

Hughes, K. L., Masterlark, T., & Mooney, W. D. (2010). Poroelastic stress-triggering of the 2005 M8. 7 Nias earthquake by the 2004 M9. 2 Sumatra–Andaman earthquake. *Earth and Planetary Science Letters*, 293(3-4), 289-299.

Idris, Y., Cummins, P., Rusydy, I., Muksin, U., Syamsidik, Habibie, M. Y., & Meilianda, E. (2019). Post-earthquake damage assessment after the 6.5 mw earthquake on December, 7th 2016 in Pidie Jaya, Indonesia. *Journal of Earthquake Engineering*, 1-18.

Irwandi, I., Muksin, U., & Simanjuntak, A. V. (2021, January). Probabilistic seismic hazard map analysis for Aceh Tenggara district and microzonation for Kutacane city. *In IOP Conference Series: Earth and Environmental Science* (Vol. 630, No. 1, p. 012001). IOP Publishing.

Ito, T., Gunawan, E., Kimata, F., Tabei, T., Simons, M., Meilano, I., Irwani, N., & Sugiyanto, D. (2012). Isolating along-strike variations in the depth extent of shallow creep and fault locking on the northern Great Sumatran Fault. *Journal of Geophysical Research: Solid Earth*, 117(B6).

Kagan, Y. Y. (2004). Short-term properties of earthquake catalogs and models of earthquake source. *Bulletin of the Seismological Society of America*, 94(4), 1207-1228.

Khan, P. K., Shamim, S., Mohanty, S. P., & Aggarwal, S. K. (2020). Change of stress patterns during 2004 MW 9.3 off-Sumatra mega-event: Insights from ridge–trench interaction for plate margin deformation. *Geological Journal*, 55(1), 372-389.

Khrepy, S. E., Koulakov, I., Al-Arifi, N., & Petrunin, A. G. (2016). Seismic structure beneath the Gulf of Aqaba and adjacent areas based on the tomographic inversion of regional earthquake data. *Solid Earth*, 7(3), 965-978.

Koulakov, I., Maksotova, G., Mukhopadhyay, S., Raoof, J., Kayal, J. R., Jakovlev, A., & Vasilevsky, A. (2015). Variations of the crustal thickness in Nepal Himalayas based on tomographic inversion of regional earthquake data. *Solid Earth*, 6(1), 207-216.

Lange, D., Tilmann, F., Henstock, T., Rietbrock, A., Natawidjaja, D., & Kopp, H. (2018). Structure of the central Sumatran subduction zone revealed by local earthquake travel-time tomography using an amphibious network. *Solid Earth*, 9, 1035-1049.

Langenbruch, C., Weingarten, M., & Zoback, M. D. (2018). Physics-based forecasting of man-made earthquake hazards in Oklahoma and

Kansas. *Nature communications*, 9(1), 1-10.

Lay, T., Kanamori, H., Ammon, C. J., Nettles, M., Ward, S. N., Aster, R. C., ... & Sipkin, S. (2005). The great Sumatra-Andaman earthquake of 26 December 2004. *Science*, 308(5725), 1127-1133.

Liu, S., Suardi, I., Yang, D., Wei, S., & Tong, P. (2018). Teleseismic traveltime tomography of northern Sumatra. *Geophysical Research Letters*, 45(24), 13-231.

Lu, C., Grand, S. P., Lai, H., & Garnero, E. J. (2019). TX2019slab: A new P and S tomography model incorporating subducting slabs. *Journal of Geophysical Research: Solid Earth*, 124(11), 11549-11567.

McCaffrey, R. (2009). The tectonic framework of the Sumatran subduction zone. *Annual Review of Earth and Planetary Sciences*, 37, 345-366.

Meltzner, A. J., Sieh, K., Chiang, H. W., Wu, C. C., Tsang, L. L., Shen, C. C., ... & Briggs, R. W. (2015). Time-varying interseismic strain rates and similar seismic ruptures on the Nias–Simeulue patch of the Sunda megathrust. *Quaternary Science Reviews*, 122, 258-281.

Meng, L., Ampuero, J. P., Stock, J., Duputel, Z., Luo, Y., & Tsai, V. C. (2012). Earthquake in a maze: Compressional rupture branching during the 2012 Mw 8.6 Sumatra earthquake. *Science*, 337(6095), 724-726.

Mueller, C. S. (2019). Earthquake catalogs for the USGS national seismic hazard maps. *Seismological Research Letters*, 90(1), 251-261.

Muksin, U., Bauer, K., Muzli, M., Ryberg, T., Nurdin, I., Masturiyono, M., & Weber, M. (2019). AcehSeis project provides insights into the detailed seismicity distribution and relation to fault structures in Central Aceh, Northern Sumatra. *Journal of Asian Earth Sciences*, 171, 20-27.

Muzli, M., Umar, M., Nugraha, A. D., Bradley, K. E., Widiyantoro, S., Erbas, K., Jousset, P., Rohadi, S., Irwandi, N., & Wei, S. (2018). The 2016 Mw 6.5 Pidie Jaya, Aceh, North Sumatra, earthquake: reactivation of an unidentified sinistral fault in a region of distributed deformation. *Seismological Research Letters*, 89(5), 1761-1772.

Omang, A., Cummins, P. R., Robinson, D., & Hidayati, S. (2017). Sensitivity analysis for probabilistic seismic hazard analysis (PSHA) in the Aceh Fault Segment, *Indonesia. Geological Society*, London, Special Publications, 441(1), 121-131.

Pasari, S. (2019). Nowcasting earthquakes in the Bay of Bengal region. *Pure and Applied Geophysics*, 176(4), 1417-1432.

Pasari, S., Simanjuntak, A. V., Mehta, A., & Sharma, Y. (2021). A synoptic view of the natural time distribution and contemporary earthquake hazards in Sumatra, Indonesia. *Natural Hazards*, 1-13.

Peña, C., Heidbach, O., Moreno, M., Bedford, J., Ziegler, M., Tassara, A., & Oncken, O. (2020). Impact of power-law rheology on the viscoelastic relaxation pattern and afterslip distribution following the 2010 Mw 8.8

Maule earthquake. *Earth and Planetary Science Letters*, 542, 116292.

Qadariah, Q., Simanjuntak, A. V., & Umar, M. (2018). Analysis of Focal Mechanisms Using Waveform Inversion; Case Study of Pidie Jaya Earthquake December 7, 2016. *Journal of Aceh Physics Society*, 7(3), 127-132.

Salman, R., Lindsey, E. O., Feng, L., Bradley, K., Wei, S., Wang, T., ... & Hill, E. M. (2020). Structural controls on rupture extent of recent Sumatran Fault Zone earthquakes, Indonesia. *Journal of Geophysical Research: Solid Earth*, 125(2), e2019JB018101.

Sieh, K., & Natawidjaja, D. (2000). Neotectonics of the Sumatran fault, Indonesia. *Journal of Geophysical Research: Solid Earth*, 105(B12), 28295-28326.

Sieh, K., Natawidjaja, D. H., Meltzner, A. J., Shen, C. C., Cheng, H., Li, K. S., ... & Edwards, R. L. (2008). Earthquake supercycles inferred from sea-level changes recorded in the corals of West Sumatra. *Science*, 322(5908), 1674-1678.

Sgambato, C., Walker, J. P. F., Mildon, Z. K., & Roberts, G. P. (2020). Stress loading history of earthquake faults influenced by fault/shear zone geometry and Coulomb pre-stress. *Scientific reports*, 10(1), 1-10.

Simanjuntak, A. V., Muksin, U., & Rahmayani, F. (2018, May). Microtremor survey to investigate seismic vulnerability around the Seulimum Fault, Aceh Besar-Indonesia. *In IOP Conference Series: Materials Science and Engineering* (Vol. 352, No. 1, p. 012046). IOP Publishing.

Simanjuntak, A. V., Muksin, U., & Setiawan, Y. (2019, June). Source Mechanism Analysis By Using Tensor Moment Inversion (Study Case: Pidie Jaya Earthquake in 2016 December 7th). *In IOP Conference Series: Earth and Environmental Science* (Vol. 273, No. 1, p. 012021). IOP Publishing.

Simanjuntak, A. V. H., Asnawi, Y., Umar, M., Rizal, S., & Syukri, M. (2020). A Microtremor Survey to Identify Seismic Vulnerability Around Banda Aceh Using HVSR Analysis. *Elkawnie: Journal of Islamic Science and Technology*, 6(2), 342-358.

Simanjuntak, A. V., & Olymphia, O. (2017). Perbandingan Energi Gempa Bumi Utama dan Susulan (Studi Kasus: Gempa Subduksi Pulau Sumatera dan Jawa). *Jurnal Fisika Flux: Jurnal Ilmiah Fisika FMIPA Universitas Lambung Mangkurat*, 14(1), 19-26.

Syamsidik, Tursina, Meutia, A., Al'ala, M., Fahmi, M., & Meilianda, E. (2017). Numerical simulations of impacts of the 2004 Indian Ocean Tsunami on coastal morphological changes around the Ulee Lheue Bay of Aceh, Indonesia. *Journal of Earthquake and Tsunami*, 11(01), 1740005.

Toda, S., Stein, R. S., Richards-Dinger, K., & Bozkurt, S. B. (2005). Forecasting the evolution of seismicity in southern California: Animations built on earthquake stress transfer. *Journal of Geophysical Research: Solid*

Earth, 110(B5).

Tsang, L. L., Meltzner, A. J., Hill, E. M., Freymueller, J. T., & Sieh, K. (2015). A paleogeodetic record of variable interseismic rates and megathrust coupling at Simeulue Island, Sumatra. *Geophysical Research Letters*, 42(24), 10-585.

van der Hist, R., Engdahl, R., Spakman, W., & Nolet, G. (1991). Tomographic imaging of subducted lithosphere below northwest Pacific island arcs. *Nature*, 353(6339), 37-43

Wesnousky, S. G. (1994). The Gutenberg-Richter or characteristic earthquake distribution, which is it?. *Bulletin of the Seismological Society of America*, 84(6), 1940-1959.

Zhao, D. (2004). Global tomographic images of mantle plumes and subducting slabs: insight into deep Earth dynamics. *Physics of the Earth and Planetary Interiors*, 146(1-2), 3-34.

Zhuang, J., Ogata, Y., & Vere-Jones, D. (2002). Stochastic declustering of space-time earthquake occurrences. *Journal of the American Statistical Association*, 97(458), 369-380.